Transcription factor E4F1 is essential for epidermal stem cell maintenance and skin homeostasis

Matthieu Lacroix[a,b,c,d,e,1], Julie Caramel[a,b,c,1], Perrine Goguet-Rubio[c,d], Laetitia K. Linares[c,d], Soline Estrach[f], Elodie Hatchi[a,b,c], Geneviève Rodier[a,b,c], Gwendaline Lledo[c,d], Carine de Bettignies[a,b,c,d], Amélie Thépot[g], Céline Deraison[e], Karim Chébli[a,b,c], Alain Hovnanian[e,2], Pierre Hainaut[g], Pierre Dubus[h], Claude Sardet[a,b,c,3], and Laurent Le Cam[a,b,c,d,3]

[a]Institut de Génétique Moléculaire de Montpellier, UMR5535, Centre National de la Recherche Scientifique, 34293 Montpellier, France; [b]Université Montpellier 2, Montpellier 34095 Cedex 5, France; [c]Université Montpellier 1, 34967 Montpellier Cedex 2, France; [d]Institut de Recherche en Cancérologie de Montpellier, Centre Régional de Lutte contre le Cancer Val d'Aurelle, Institut National de la Santé et de la Recherche Médicale U896, 34298 Montpellier, France; [f]Faculté de Médecine, Institut National de la Santé et de la Recherche Médicale U634, 06107 Nice, France; [g]International Agency for Research on Cancer, 69008 Lyon, France; [e]Institut National de la Santé et de la Recherche Médicale U563, F-31300 Toulouse, France; and [h]EA2406 Université Victor Segalen Bordeaux 2, 33076 Bordeaux, France

Edited* by Robert A. Weinberg, Whitehead Institute for Biomedical Research, Cambridge, MA, and approved October 26, 2010 (received for review July 15, 2010)

A growing body of evidence suggests that the multifunctional protein E4F1 is involved in signaling pathways that play essential roles during normal development and tumorigenesis. We generated *E4F1* conditional knockout mice to address E4F1 functions in vivo in newborn and adult skin. *E4F1* inactivation in the entire skin or in the basal compartment of the epidermis induces skin homeostasis defects, as evidenced by transient hyperplasia in the interfollicular epithelium and alteration of keratinocyte differentiation, followed by loss of cellularity in the epidermis and severe skin ulcerations. *E4F1* depletion alters clonogenic activity of epidermal stem cells (ESCs) ex vivo and ends in exhaustion of the ESC pool in vivo, indicating that the lesions observed in the *E4F1* mutant skin result, at least in part, from cell-autonomous alterations in ESC maintenance. The clonogenic potential of *E4F1* KO ESCs is rescued by Bmi1 overexpression or by Ink4a/Arf or p53 depletion. Skin phenotype of *E4F1* KO mice is also delayed in animals with *Ink4a/Arf* and *E4F1* compound gene deficiencies. Our data identify a regulatory axis essential for ESC-dependent skin homeostasis implicating E4F1 and the Bmi1–Arf–p53 pathway.

mouse model | bulge | long term label retaining cells | wound healing

E4F1 is an ubiquitously expressed transcription factor of the Gli–Kruppel family that was identified as a cellular target of the adenoviral oncoprotein E1A (1). Although several cellular targets of E1A (e.g., E2F/pRB, CBP/p300, PCAF, CtBP, ATF/Creb) have been studied extensively and are recognized as central regulators of cell proliferation and survival, the biological functions of E4F1 remain poorly investigated. E4F1 is a multifunctional protein with transcriptional and atypical ubiquitin E3 ligase activities. E4F1-mediated ubiquitylation modulates the p53 transcriptional activities involved in alternative cell fates, either growth arrest or apoptosis (2). The idea that E4F1 plays an important role in the p53 pathway is reinforced by other reports showing that E4F1 interacts directly not only with p53 itself (2, 3) but also with regulators/effectors of this pathway, including $p14^{ARF}$ (4), the polycomb member Bmi1 (5), and the p53 target gene FHL2 (6). However, the functions of E4F1 likely extend beyond the regulation of p53, however. Indeed, physical interactions between E4F1 and components of other oncogenic pathways, including RASSF1A, pRB, HMGA2, and Smad4, have been reported (7–10).

Using a gene targeting approach in mice, we previously showed that *E4F1* constitutive inactivation results in embryonic lethality near the time of implantation. *E4F1 KO* blastocysts in culture exhibit mitotic defects, including lagging chromosomes, chronic activation of the mitotic checkpoint, and cell death (11). More recently, shRNA-mediated partial depletion of E4F1 was shown to rescue hematopoietic stem cell (HSC) exhaustion in mouse resulting from inactivation of the polycomb member *Bmi1* (5), suggesting an important role for E4F1 in HSC homeostasis. To date, little information is available regarding in vivo functions of E4F1 in adult tissues. In the present work, we generated mouse strains to explore the roles of E4F1 in skin homeostasis.

Constant renewal of the interfollicular epithelium (IFE) and of hair follicles (HFs) relies on the recruitment of epidermal stem cells (ESCs) located in the basal layer of the IFE and in the bulge region of the HFs, respectively. ESCs fuel the highly proliferative transit amplifying compartments (TACs) in the basal layer of the IFE and in the bulbs of HFs. TAC cells then embark on differentiation programs to generate the spinous, granular, and cornified layers in the IFE or the different lineages of mature HFs (12–14). Several essential molecular circuitries that orchestrate ESC maintenance, including p63-, BMP-, TGF-β–, Wnt/β-catenin–, and Notch-initiated signaling cascades, have been described (12, 15, 16).

Here we report that inactivation of *E4F1* in the entire skin or in the basal compartment of the epidermis results in severe epidermal defects in both neonatal and adult mice, revealing an as-yet unidentified regulatory axis essential for ESC-dependent skin homeostasis implicating E4F1 and the Bmi1–Ink4a/Arf–p53 pathway.

Results

***E4F1* KO Induces Transient Hyperplasia in the Epidermis, Followed by Permanent Loss of Epidermal Cells and Severe Skin Ulcerations.** Immunohistochemistry (IHC) analyses of murine and human skin sections demonstrated nuclear expression of E4F1 in the basal and suprabasal layers of the IFE, as well as in the bulb and bulge regions of the HFs (Fig. 1*A*). To address the role of E4F1 in skin homeostasis, we generated mouse models with conditional homozygote deletion of the *E4F1* gene in the entire skin or in the epidermis only. In short, we generated $E4F1^{-/flox}$ mice (Fig. S1) and intercrossed them with $Cre\text{-}ER^{T2\ KI/KI}$ mice (*RERT*), which ubiquitously express tamoxifen-inducible Cre recombinase-ER^{T2} fusion protein (17). Topical applications of 4-hydroxytamoxifen (4OHT) on the tail skin or on a shaved area of the back skin of adult $E4F1^{-/flox}$;*RERT* mice resulted in efficient recombination of the *E4F1* locus in the skin, as monitored in genomic DNA, mRNA,

Author contributions: M.L., J.C., C.S., and L.L.C. designed research; M.L., J.C., P.G.-R., L.K.L., S.E., E.H., G.R., G.L., C.d.B., A.T., K.C., and L.L.C. performed research; S.E., G.R., C.d.B., A.H., P.H., and P.D. contributed new reagents/analytic tools; M.L., J.C., C.D., A.H., P.H., P.D., C.S., and L.L.C. analyzed data; and C.S. and L.L.C. wrote the paper.

The authors declare no conflict of interest.

*This Direct Submission article had a prearranged editor.

[1]M.L. and J.C. contributed equally to this work.

[2]Present address: Département de Génétique, CHU Necker-Enfants Malades, 75015 Paris, France.

[3]To whom correspondence may be addressed. E-mail: claude.sardet@igmm.cnrs.fr or laurent.lecam@inserm.fr.

This article contains supporting information online at www.pnas.org/lookup/suppl/doi:10.1073/pnas.1010167107/-/DCSupplemental.

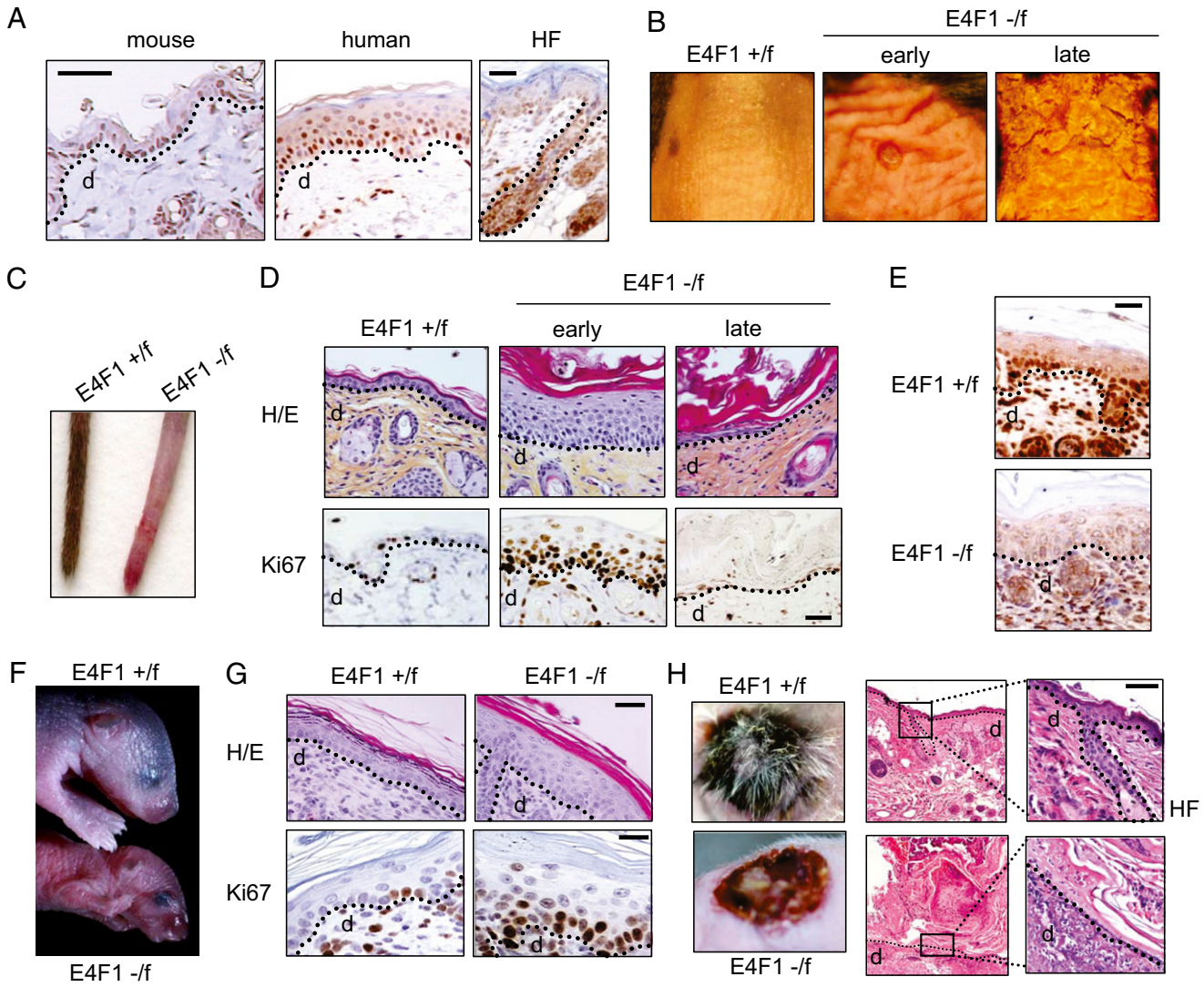

Fig. 1. *E4F1* KO triggers transient hyperplasia of the epidermis, followed by permanent loss of epidermal cells and severe skin ulcerations. (*A*) IHC analysis of E4F1 expression in human skin or murine back skin and HFs. (Scale bar: 40 μm.) The dotted line indicates the dermis (d)–epidermis junction. (*B*) Macroscopic alterations of back skin of adult *E4F1*$^{-/flox}$*;RERT* mice 7 (early) or 15 d (late) after Cre-mediated *E4F1* KO. (*C*) *E4F1*^{flox}*; RERT* tails at late time points (6 wk) after 4OHT application. (*D*) H&E staining (*Upper*) and Ki67 IHC analyses (*Lower*) of dorsal skin sections prepared from 4OHT-treated *E4F1*$^{-/flox}$*;RERT* or *E4F1*$^{+/flox}$*; RERT* control adult mice at early and late time points. (Scale bar: 20 μm.) (*E*) IHC analysis of dorsal skin sections from *E4F1*$^{+/flox}$*;K5-Cre* and *E4F1*$^{-/flox}$*;K5-Cre* neonates using anti-E4F1 antibody. (Scale bar: 40 μm.) (*F*) *E4F1*$^{+/flox}$ and *E4F1*$^{-/flox}$*;K5-Cre* neonates (P4) showing acute symptoms of dehydration. (*G*) H&E staining (*Upper*) and Ki67 IHC analysis (*Lower*) of dorsal skin sections prepared from *E4F1*^{flox}*;K5-Cre* P4 neonates. (Scale bar: 20 μm.) (*H*) H&E-stained sections of back skin from *E4F1*$^{+/flox}$*;K5* or *E4F1*$^{-/flox}$*;K5-Cre* P1 neonates at 2 wk after engraftment onto recipient nude mice. (Scale bar: 40 μm.)

and protein samples prepared from treated areas (Fig. S1). Between 1 and 2 wk after 4OHT treatment, E4F1-depleted back skin thickened and became wrinkled and ruffled. These early lesions evolved 1–2 wk later into severe skin ulcerative lesions (Fig. 1*B*). *E4F1* KO in unshaved skin tails of *E4F1*$^{-/flox}$*;RERT* mice resulted in complete alopecia by 6 wk after 4OHT application (Fig. 1*C*). Histological analyses revealed that skin thickening resulted from massive hyperplasia of the epidermis with increased cellularity in the IFE and the infundibulum (Fig. 1*D*). Consistent with hyperplasia, an abnormal proportion of epidermal cells proliferated in *E4F1* KO skin, as indicated by increased Ki67 (Fig. 1*D*) and BrdU (Fig. S2) immunostainings of skin sections. This phenotype was skin-autonomous, as demonstrated by the recapitulation of similar hyperplasia on *E4F1*$^{-/flox}$*;RERT* neonatal back skin engrafted onto nude mice (Fig. S3). At later time points (3–4 wk after 4OHT treatment), the initial hyperplasia of *E4F1 KO;RERT* skin was followed by broad disorganization of the IFE and massive hyperkeratosis, associated with partial or complete loss of cellularity in the IFE (Fig. 1*D*). Of note, sebaceous glands appeared to be unaltered in *E4F1* KO skin, as suggested by Nile red staining on whole-mount experiments and H&E coloration (Fig. S4).

To confirm that this phenotype resulted from epidermis-specific defects, we next crossed *E4F1*$^{-/flox}$ mice with *keratin 5 (K5)-Cre* transgenic mice expressing Cre in the basal cell layer of the epidermis from E15.5 onward (18). The *E4F1*$^{-/flox}$*;K5-Cre* neonates exhibited efficient *E4F1* KO in the epidermis (Fig. 1*E* and Fig. S1). At 3–4 d after birth, these mice developed epidermal hyperplasia and died exhibiting symptoms of acute dehydration (Fig. 1*F*). As in *E4F1*$^{-/flox}$*;RERT* skin, hyperplasia was observed in *E4F1*$^{-/flox}$*; K5-Cre* epidermis was associated with hyperproliferation and higher mitotic index of epidermal basal cells, as shown by increased Ki67 (Fig. 1*G*) and phospho-histone H3 (Ser10; PHH3) staining (Fig. S5*D*). Of note, we previously showed that *E4F1* KO blastocysts exhibited abnormal mitotic figures associated with increased PHH3 staining (11). These abnormalities were not observed in *E4F1* KO epidermal basal cells, indicating that the

increased mitotic index likely reflected the overproliferation of basal cells, rather than mitotic progression defects.

To bypass neonatal lethality, we engrafted *E4F1 KO;K5-Cre* skin onto nude mice. At 2 wk after engraftment, the *E4F1 KO* grafts failed to regenerate a normal epidermis and exhibited marked epidermal hypocellularity, hyperkeratosis, severe ulcerative lesions, and lack of HFs (Fig. 1*H*), similar to the late phenotype of the *E4F1*$^{-/flox}$*;RERT* mice. Taken together, these data show that *E4F1* KO results in transient hyperplasia and ultimately leads to a permanent loss of epidermal cells in the IFE and HFs.

***E4F1* KO Results in Expansion of Epidermal Basal Cells and Abnormal Differentiation in Vivo.** In both 4OHT-treated *E4F1*$^{-/flox}$*;RERT* and *E4F1*$^{-/flox}$*;K5-Cre* epidermis, cells of the hyperplasic IFE stained positive for basal cell–specific K14 and integrin-α6 markers (Fig. 2*A* and Fig. S6*A*). Expression of these markers extended to upper cellular layers, in contrast to the normal IFE of control animals, in which marker expression was restricted to the basal cell layer. *E4F1*-floxed IFE also massively expressed K6 (Fig. 2*B* and Fig. S6*B*), which is normally restricted to sweat glands and HFs in normal skin but can be expressed in IFE undergoing abnormal proliferation or wound healing (19). We also noticed an absence of suprabasal and granular layers in KO epidermis, as illustrated by the lack of expression of early (K1 and K10) and late (involucrin, loricrin, filaggrin) differentiation markers (Fig. 2*B* and Fig. S6*B*). Of note, no significant cell death was observed in hyperplasic lesions, suggesting that hyperproliferative cells had finally undergone an abnormal differentiation program of stratification, rather than apoptosis, leading to the observed hyperkeratosis. These data indicate that *E4F1* KO in the IFE results in massive expansion of keratinocytes with basal/TAC properties and also alters the differentiation of epidermal lineages.

***E4F1* KO Induces Epidermal Stem Cell Defects.** Several scenarios could explain how *E4F1* KO leads to a transient expansion of the basal/TAC compartment of the epidermis. First, the overproliferation of basal cells could reflect an increase in the intrinsic proliferation capability of basal/TAC keratinocytes. This scenario is unlikely, however, given that *E4F1* KO primary keratinocytes isolated from *E4F1*$^{-/flox}$*;K5-Cre* p1 neonates did not recapitulate in culture the overproliferation observed in skin sections, as demonstrated by BrdU/propidium iodide (PI) or PHH3/PI labeling (Fig. S5 *A* and *C*). Similar findings were seen in primary human keratinocytes upon shRNA-mediated depletion of endogenous *E4F1* (Fig. S5*B*). These data, together with the withering and transient aspect of the hypertrophy phenotypes, led us to investigate an alternative hypothesis involving perturbations of resident ESCs. Thus, inactivation in the epidermis of key signaling molecules, including Rac1, Myc, Smad4, and NFATC1, causes ESCs to exit their normal microenvironment to enter into the TACs, where they become transiently proliferating keratinocytes on exposure to natural promitogenic signals present in this amplification compartment (20–24). This results in transient hyperplasia, followed by a permanent exhaustion of the ESC pool. To examine this scenario, we first performed clonogenic assays with primary keratinocytes isolated from in vivo recombined hyperplasic regions of *E4F1*$^{-/flox}$*;RERT* adult mice, *E4F1*$^{-/flox}$*;K5-Cre* p1 neonates, and control littermates. After 10–15 d in culture, typical holoclones, corresponding to the long-term clonal outgrowth of epidermal cells with stem cell properties (25, 26), were detected in controls, but not under *E4F1* KO conditions (Fig. 3*A*). Importantly, similar reduction was recapitulated when *E4F1* KO was induced ex vivo by adding 4OHT in the culture medium of *E4F1*$^{-/flox}$*;RERT* cells (Fig. 3*A*), demonstrating that these defects are stem cell autonomous. Similarly, shRNA-mediated partial depletion of E4F1 in primary human keratinocytes resulted in a 3-fold reduction in the number of holoclones (Fig. 3*B*).

We next investigated whether *E4F1* KO also resulted in exhaustion of the stem cell pool in vivo by analyzing the expression of various ESC markers. FACscan flow cytometry analyses revealed that *E4F1*$^{-/flox}$*;K5-Cre* neonatal epidermis contained fewer ESCs coexpressing CD34 and higher levels of α6-integrin (CD34^{+}/α6^{high}) compared with control epidermis (8% ± 2% vs. 1.5% ± 1%; $n = 3$) (Fig. 3*C*). Similarly, immunostainings of back skin sections and whole mounts of tail epidermis showed significant reductions in HF bulge markers CD34 and K15 in adult *E4F1*$^{-/flox}$*;RERT* animals at 4–6 wk after *E4F1* KO (Fig. 3*D* and Fig. S7*A*).

We also crossed *E4F1*$^{-/flox}$*;RERT* animals with *K15-EGFP* transgenic mice expressing the GFP reporter under the control of the K15 promoter (27). In 7- to 12-wk-old *K15-GFP;E4F1*$^{+/flox}$*;RERT* control animals, GFP expression was restricted to the bulge region of unsynchronized HFs. In contrast, a complete loss of GFP-positive cells was observed at 4–6 wk after *E4F1* KO, confirming the exhaustion of HF ESCs (Fig. 3*E*). Finally, we tracked HF bulge/ESCs as BrdU long-term retaining cells (LRCs) using an in vivo labeling protocol that marks self-renewing and multipotent epidermal cells (26, 28). *E4F1*$^{-/flox}$*;RERT* and *E4F1*$^{+/flox}$*;RERT* neonates were injected with BrdU, and after a chase period of 3 months, the poorly proliferative adult ESCs were identified on whole mounts of tail epidermis as BrdU-positive LRCs. At 2–3 wk after *E4F1* KO, the LRC zone was extended, and increased numbers of LRCs were colabeled with Ki67 in *E4F1* KO HFs compared with control HFs (Fig. 3*F*, early and Fig. S7*B*), suggesting that *E4F1* KO induced transient proliferation of HF ESCs. At later time points (6 wk), although LRCs were still restricted to the HF bulges in controls, BrdU staining finally disappeared in the *E4F1* KO HFs (Fig. 3F, late), further suggesting that *E4F1* KO results in exhaustion of the ESC pool. ESCs also play a major role in regenerating hairy skin after injury (26). Accordingly, wound healing was strongly altered in *E4F1* KO skin (Fig. S8). Taken together, these findings indicate that *E4F1* is essential for ESC maintenance in vivo and ex vivo, and strongly suggest that the hyperplasia and subsequent loss of cellularity of *E4F1* KO epidermis are due primarily to cell-autonomous perturbations of the ESC pool that supplies TAC compartments.

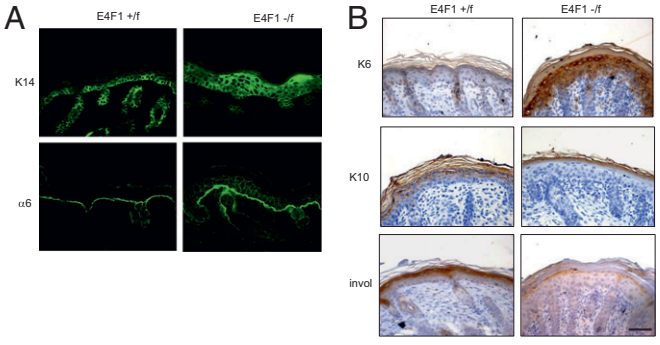

Fig. 2. *E4F1* KO results in expansion of the basal cell compartment of the epidermis and in abnormal keratinocyte differentiation in vivo. (*A*) Immunostainings of dorsal skin sections from *E4F1*$^{+/flox}$ and *E4F1*$^{-/flox}$*;K5-Cre* neonates with anti-K14 and anti–α6 integrin antibodies. (*B*) IHC analysis of dorsal skin sections from *E4F1*$^{+/flox}$ and *E4F1*$^{-/flox}$*;K5-Cre* neonates with anti-K6, anti-K10, or anti-involucrin (invol) antibodies. (Scale bar: 40 μm.)

Down-Regulation of the Bmi1-Ink4a/Arf-p53 Axis Partly Rescues ESC Clonogenic Potential and Skin Lesions of *E4F1 KO*. We next addressed the molecular pathway by which E4F1 could regulate ESC maintenance. E4F1 associates with the polycomb member Bmi1 and the tumor suppressors Arf, p53, and pRb (2–5, 8). Although some evidence suggests that these factors have independent functions, they define a functional cascade with Bmi1 triggering the repression of the *Ink4a/Arf* locus, whose products, p19^{Arf} and p16^{Ink4a}, act as potent inhibitors of p53- and pRb-dependent activities, respectively (29). Repression of *Ink4a/Arf* expression is considered a central event in stem cell renewal in several tissues, including the epidermis (30–34). Strikingly, *E4F1* KO keratino-

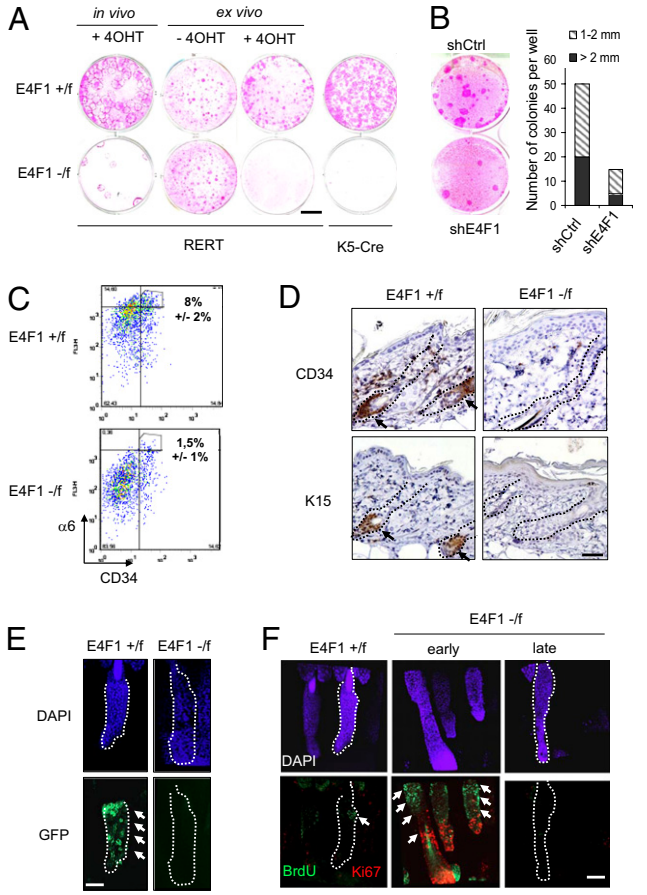

Fig. 3. *E4F1* KO results in ESC exhaustion in vivo and ex vivo. (*A*) Clonogenic assays performed with primary murine keratinocytes prepared from back skin of *E4F1^{flox};RERT* adult mice 6 d after 4OHT applications (in vivo), from *E4F1^{flox};RERT* neonatal skins and treated with 4OHT in culture medium (ex vivo), or from *E4F1^{flox};K5-Cre* neonates (P1). Rhodamine B staining was performed after 15 d of culture. Data shown are representative of experiments performed in duplicate and repeated at least three times. (Scale bar: 1 cm.) (*B*) (*Left*) Clonogenic assays performed with human primary keratinocytes transduced with retroviral vectors expressing shRNAs targeting either human E4F1 (shE4F1) or a nonrelevant sequence (shCtrl). (*Right*) Quantification of the total number and size (diameter, in mm) of clones from three independent experiments. (*C*) FACScan analyses of primary keratinocytes isolated from *E4F1^{flox};K5-Cre* P3 neonates after α6-integrin and CD34 immunostainings. The percentage of α6^{high}/CD34^{+} epidermal stem cells is indicated (average of three independent experiments ± SD). (*D*) IHC analyses of back skin sections from *E4F1^{flox};RERT* adult mice at 3 wk after 4OHT application with antibodies directed against CD34 and K15. Arrows indicate K15- or CD34-positive stem cells located in the bulge region of HFs. (Scale bar: 80 μm.) (*E*) Whole mounts of tail epidermis prepared from *E4F1^{flox};RERT;K15-GFP* mice at 4 wk after 4OHT application. White arrows indicate K15-GFP^{+} ESCs located in the bulge region of HFs in control animals (*E4F1$^{+/flox}$*) treated with 4OHT (*Left*). (Scale bar: 80 μm.) (*F*) Analyses of BrdU LRCs in whole mounts of tail epidermis prepared from 16-wk-old mice. Anti-BrdU (green) and anti-Ki67 (red) immunostainings of *E4F1$^{+/flox}$;RERT* and *E4F1$^{-/flox}$;RERT* HFs at 3 wk (early) or 6 wk (late) after *E4F1* KO showing transient hyperproliferation followed by a loss of LRCs (white arrows). LRCs are located in the bulge region of HFs from control skin (*E4F1$^{+/flox}$*) treated with 4OHT for 6 wk. (Scale bar: 80 μm.)

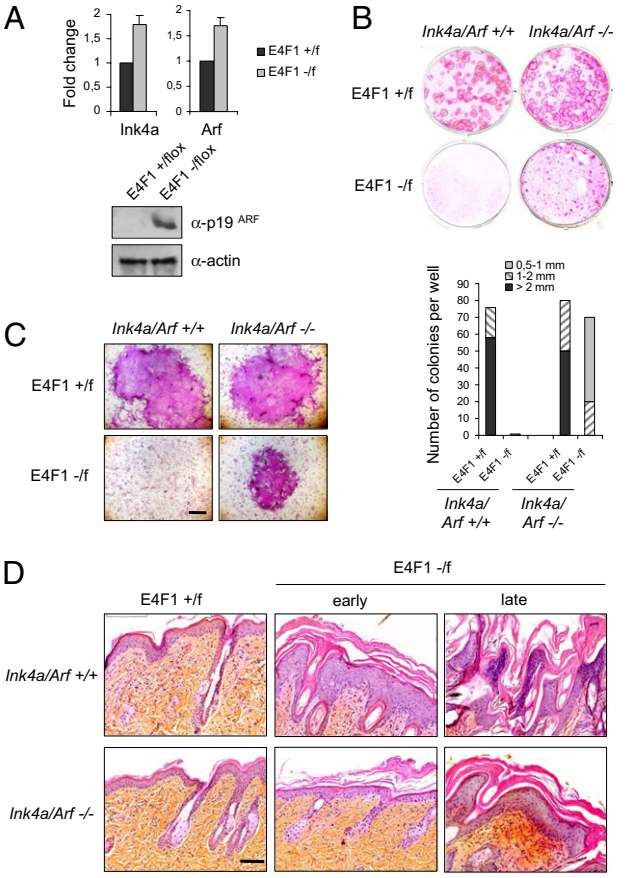

Fig. 4. Deletion of the *Ink4a/Arf* locus partially rescues *E4F1* KO skin defects in vivo and ex vivo. (*A*) Quantitative RT-PCR analyses of *Ink4a* and *Arf* mRNA levels (*Upper*) and p19^{ARF} immunoblot analyses (*Lower*) performed on *E4F1$^{+/flox}$* or *E4F1$^{-/flox}$;K5-Cre* freshly isolated primary keratinocytes. (*B*) Clonogenic assays performed with *E4F1^{flox};RERT;Ink4a/Arf$^{-/-}$* or *E4F1^{flox};RERT;Ink4a/Arf$^{+/+}$* primary keratinocytes in the presence of 4OHT. Shown is one representative experiment of three independent experiments performed in duplicate. Quantitative analyses of the number and size (diameter, in mm) of clones was performed after 15 d in culture. (*C*) High-magnification photograph of representative clones. (Scale bar: 0.5 mm.) (*D*) H&E staining of dorsal skin sections prepared from 4OHT-treated *E4F1^{flox};RERT;Ink4a/Arf$^{+/+}$* 12-wk-old mice and *E4F1^{flox};RERT;Ink4a/Arf$^{-/-}$* mice.

cytes exhibited increased levels of *Ink4a* and *Arf* mRNA and p19^{Arf} protein compared with control cells (Fig. 4*A*). To assess the impact of this deregulation in the *E4F1* KO phenotype, we generated *E4F1^{flox};RERT;Ink4a/Arf$^{-/-}$* compound mice. Clonogenic assays performed with keratinocytes isolated from these animals showed that *Ink4a/Arf* KO partly restored long-term outgrowth of *E4F1* KO ESCs ex vivo (Fig. 4 *B* and *C*). Accordingly, the in vivo skin phenotype induced by *E4F1* KO was delayed in these animals. The epidermal hyperplasia was almost undetectable at early time points after 4OHT treatment (Fig. 4*D*, early), but moderate hyperplasia and hyperkeratosis were evident at later time points (Fig. 4*D*, late).

A partial rescue of the clonogenic potential of *E4F1* KO ESCs was also obtained on overexpression of Bmi1, a main repressor of the *Ink4a/Arf* locus (Fig. 5 *A* and *C*), providing additional evidence for a role of the Ink4a/Arf–pRb/p53 cascades in the *E4F1* KO phenotype. To assess which *Ink4a/Arf* downstream targets were involved, we repeated clonogenic assays on shRNA-mediated depletion of either murine *RB1* or *p53* (Fig. 5 *B* and *C*). p53 depletion, but not pRb depletion, restored clonal outgrowth of *E4F1 KO* keratinocytes, highlighting the role of the Bmi1-Arf-p53 axis rather than the Bmi1-p16-pRb axis in *E4F1 KO* skin phenotypes. Of note, *E4F1* KO rescued clones that developed on inactivation of *Ink4a/Arf*, depletion of p53, or overexpression of Bmi1 were significantly smaller than those growing from control cells (Figs. 4 *B* and *C* and 5 *A* and *B*), suggesting that E4F1 also might also impinge on other molecular circuitries that orchestrate ESC maintenance.

Taken together, our findings provide evidence that E4F1 is essential for ESC-dependent skin homeostasis and identify a regulatory axis involved in this process, implicating Bmi1 and the Arf–p53 pathway.

GENETICS

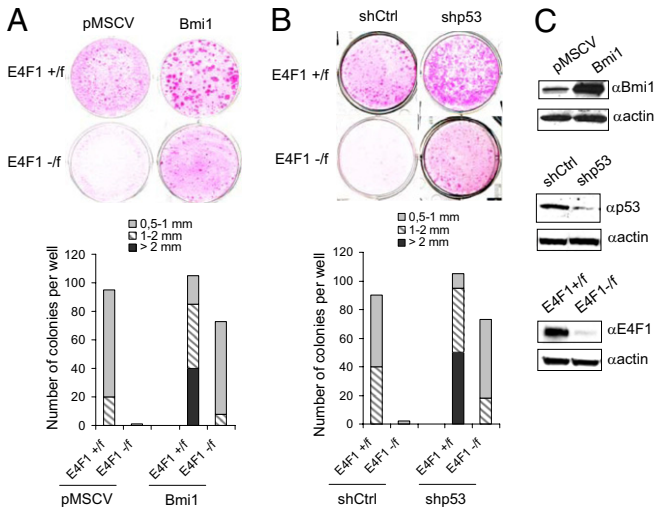

Fig. 5. Down-regulation of the Bmi1-Arf-p53 axis rescues *E4F1* KO ESC defects. (*A*) Primary keratinocytes isolated from *E4F1^{flox};RERT* neonates were transduced with control (pMSCV) or Bmi1-encoding retroviruses (Bmi1) and used for clonogenic assays in the presence of 4OHT. (*B*) Clonogenic assays performed with *E4F1^{flox};RERT* primary keratinocytes transduced with control (shCtrl) or p53 (shp53) shRNAs encoding lentiviruses in presence of 4OHT. *A* and *B* present photographs (*Upper*) and quantifications (*Lower*) of a representative experiment. Three independent experiments were performed in duplicate. Quantitative analyses of the number and size (diameter, in mm) of clones were performed after 10 d. (*C*) Western blot analyses showing ectopic overexpression of Bmi1 in rescued *E4F1 KO* clones or shRNA-mediated depletion of p53 in rescued *E4F1 KO* clones.

Discussion

We have shown that *E4F1* KO in the epidermis leads to neonatal lethality resulting from defects in skin homeostasis. E4F1 depletion in *E4F1 KO;K5-Cre* neonates and *E4F1$^{-/flox}$;RERT* adult skin led to rapid thickening of the IFE with increased numbers of proliferative basal keratinocytes. This hyperplasia was transient, and was followed by severe disorganization and an almost complete loss of viable epithelial cell layers in the IFE and HFs. In addition, perturbations of epidermal differentiation were observed in both *E4F1* KO models. Strikingly, *E4F1* depletion in murine or human primary keratinocytes in culture did not recapitulate the overproliferation observed in skin sections, ruling out the possibility that hyperplasia originates from an intrinsic increase in the proliferative capacity of *E4F1* KO TAC keratinocytes. As has been described for other gene deficiencies in epidermis (20, 22), our data suggest that the *E4F1 KO* phenotypes resulted from cell-autonomous perturbations in resident stem cells. *E4F1* depletion in vivo or ex vivo dramatically impaired the clonogenic potential of both murine and human epidermal cell populations and resulted in a strong reduction in the expression of various ESC markers in *E4F1* KO skin. BrdU labeling of LRCs suggested that *E4F1* KO HF stem cells first exited their normal location in the bulge region of HFs to enter into a transient phase of proliferation before disappearing. Accordingly, exhaustion of the resident stem cell pool in *E4F1* KO skin ultimately led to a complete loss of cellularity in the IFE and altered wound healing.

The clonogenic potential of *E4F1* KO ESCs was restored upon targeting of the Bmi1-Ink4a/Arf-p53 axis, but not by pRb depletion, highlighting the role of the Bmi-Arf-p53 axis rather than the Bmi-p16-pRb axis in *E4F1 KO* skin phenotypes. Consistently, *E4F1* KO was correlated with increased Ink4a/ARF expression, and hyperplasia was delayed and reduced in mice with *Ink4a/Arf* and *E4F1* compound gene deficiencies. This calls into question the poorly documented physiological functions of the Bmi1-Ink4a/Arf-p53 axis in ESC homeostasis. This axis might play its usual "gatekeeper" function, notably in response to genotoxic or developmental stress, as has been reported in mice with dysfunctional telomeres (35, 36) and in *p63 KO* mice (34, 37). As has been described in other tissues, this axis also could play a role in ESC self-renewal, symmetric division, or maintenance programs, as has been reported in hematopoietic multipotent progenitors (38), neural stem cells (39), and mammary gland progenitor cells (40). This raises questions about the role of p53 (and, indirectly, of E4F1) in the epidermis, where proper columnar stratification and tissue organization are driven, at least in part, by oriented, asymmetric cell divisions (41, 42).

How E4F1 inactivation affects *Ink4a/Arf* levels also remains unclear. As a bona fide transcription factor, E4F1 might directly transactivate or might cooperate/interfere with other transcriptional regulators of the *Ink4a/Arf* locus. Consistent with this scenario, E4F1 physically interacts with Bmi1, a main repressor of this locus (5). We found that, similar to *Ink4a/Arf* inactivation, Bmi1 ectopic overexpression partly rescued the clonogenic potential of *E4F1* KO ESCs. Nevertheless, the genetic links between E4F1 and Bmi1 in stem cell maintenance are likely complex and might differ among tissues. Indeed, other investigators have shown that shRNA-mediated depletion of E4F1 rescues premature senescence of *Bmi1* KO hematopoietic stem cells in an *Ink4a/Arf*- and *p53*-independent manner (5). E4F1 might also exert other, as-yet unidentified cellular functions independent from Bmi1 and the Arf-p53 axis, as suggested by our finding that targeting the Bmi1-Arf-p53 axis did not fully restore ESC clonal outgrowth and normal skin phenotype. Thus, it could be proposed that E4F1 also impinges on other molecular circuitries that orchestrate ESC maintenance, including TGFβ/BMP-, Wnt/β-catenin–, Notch-, and p63-initiated signaling cascades (10, 12–14). Indeed, E4F1 might act as a transcriptional regulator of the *p63* gene or as a post-translational modifier of p63 activity, as has been described for p53. This is unlikely, however, given that mRNA levels of Δ*Np63* and of several hiherto described transcriptional targets of p63 (*Perp, Claudin1*, *Fibronectin1*, *Eva1*, *Runx1*, and *Redd1*) (43) remained unchanged in *E4F1* KO samples (Fig. S9). Concerning the Notch pathway, we did not detect changes in *Notch1* transcripts levels in *E4F1 KO* keratinocytes (Fig. S9), suggesting that this pathway is not directly involved in the *E4F1* KO phenotype.

In conclusion, we have provided evidence that E4F1, through its connection with the Bmi1 and the Ink4a/Arf-p53 axis, plays a role in stem cell–dependent skin homeostasis. This finding, together with reports showing that E4F1 is targeted by several oncoproteins and tumor suppressors, raise questions about E4F1's role in the development and maintenance of cancer stem cells whose presence is suspected in skin carcinoma and malignant melanoma.

Materials and Methods

***E4F1$^{-/flox}$* Mice and Experimental Treatment of Mice.** Generation of the *E4F1^{flox}* allele and of *E4F1$^{-/flox}$* mice is detailed in *SI Materials and Methods*. Experimental groups were composed of *E4F1$^{+/flox}$* or *E4F1$^{-/flox}$;RERT$^{KI/KI}$*, *E4F1$^{+/flox}$* or *E4F1$^{-/flox}$;RERT$^{KI/KI}$*; *Ink4a/Arf$^{+/+}$* or *Ink4a/Arf$^{-/-}$*, and *E4F1$^{+/flox}$* or *E4F1$^{-/flox}$;RERT$^{KI/KI}$;K15-GFP* Tg mice (17, 18, 27, 44). Compound mice were maintained on a mixed *129SvJ/DBA/C57BL/6* background, and phenotypic characterization was performed in parallel on 12- to 16-wk-old *E4F1$^{+/flox}$* and *E4F1$^{-/flox}$* littermates. *E4F1* recombination in adult *E4F1^{flox};RERT* skin was induced by four topical applications of 4OHT (in ethanol, 2 mg/day; Sigma-Aldrich) on shaved back or tail skin. For skin grafting experiments, dorsal skin from *E4F1^{flox};RERT* or *E4F1^{flox};K5-Cre* neonate donors were transplanted onto athymic nude recipient mice (Charles River) as described previously (45). For visualization of BrdU LRCs, 10-d-old mice were injected with BrdU (50 mg/kg; Sigma-Aldrich) every 12 h for a total of four injections. To achieve short-term labeling of cells undergoing DNA synthesis in vivo (for IHC experiments), BrdU (50 mg/kg) was injected i.p. 4 h before euthanasia. All experiments were approved by the University of Montpellier's Ethics Committee for Animal Welfare.

Histochemistry, Immunolabeling of Skin Sections and Whole Mounts, and Immunoblot Analysis. Immunolabeling of skin sections were as described in *SI Materials and Methods* using the following antibodies: anti-E4F1 (B-21 rabbit polyclonal, from our laboratory), anti-Ki67 (SP6; Neomarkers), anti-K6 (SPM269; Abcam), anti-K10 (PRB-159P; Covance), anti-involucrin (Sc15230;

Santa Cruz Biotechnology), anti-CD34 (RAM34; BD Pharmingen), anti-K15 (LHK15; Vector Laboratories), anti–α6-integrin (GoH3; BD Biosciences), anti-K14 (AF64; Covance), and anti-BrdU antibody (BD Biosciences). Immunoblots were probed with anti-E4F1 (8), anti-p53 (1C12; Cell Signaling), Bmi1 (F6; Millipore), anti-$p19^{ARF}$ (Ab80; Abcam), and anti–β-actin (Sigma-Aldrich). Whole mounts of tail epidermis and detection of LRCs were performed as described previously (28) and as detailed in *SI Materials and Methods*. For FACScan analyses, cells were probed with FITC-conjugated anti-CD34 (RAM34; BD Biosciences) and PE-Cy5–conjugated anti–α6-integrin antibodies.

Culture of Primary Keratinocytes and Clonogenic Assays. Murine primary keratinocytes were isolated from newborn or adult back skin, and clonogenic assays were perfomed as described in *SI Materials and Methods*. Cre-mediated recombination of *E4F1* flox alleles was achieved by adding 4OHT (1 μM) to the culture medium. Human primary keratinocytes were isolated from skin biopsy specimens in accordance with the Declaration of Helsinki and cultured as described in *SI Materials and Methods* (46).

Retroviral and Lentiviral Particle Production and Infections. Viral particles were produced as described in *SI Materials and Methods* from pMSCV-Bmi1 (29), pMKO vector encoding either control or anti human *E4F1* shRNAs, pLKO1 encoding shRNAs directed against murine RB1 or p53 (MISSION NM_011640.1–625s1c1; Sigma-Aldrich), or control irrelevant sequences.

Quantitative RT-PCR. The primers and conditions used for quantitative RT-PCR analyses are described in *SI Materials and Methods*.

ACKNOWLEDGMENTS. We thank members of L.L.C.'s and C.S.'s laboratories, C. Jacquet, E. Jouffre, and P. Cavelier, for providing technical help and critical readings; Institut de la clinique de la souris (Strasbourg) for performing injections of E4F1 flox ES cells into blastocysts; and C. Blanpain (University of Brussels, Brussels), M. Van Lohuizen (National Cancer Institute, Amsterdam), J. Jorcano and A. Ramirez (Centro de investigaciones energéticas medioambientales y tecnalogicas, Madrid), A. Gandarillas (Instituto de Formación e Investigación Marqués de Valdecilla, Santander, Spain), M. Barbacid, and M. Serrano (Centro nacional de investiganioces oncologicas, Madrid) for providing reagents and mice. Imaging and histological analyses were performed at the Montpellier Rio Imaging and Réseau d'Histologie Expérimentale de Montpellier core facilities (Montpellier), respectively. C.S. and J.C. are supported by the Agence Nationale pour la Recherche, the American Institute for Cancer Research, la Fondation pour la Recherche Médicale, and institutional supports from Centre National de la Recherche Scientifique. L.L.C. is supported by the INSERM Avenir Program, the Association pour la Recherche contre le Cancer (ARC), and the Ligue Contre le Cancer. M.L. and E.H. are supported by fellowships from ARC.

1. Raychaudhuri P, Rooney R, Nevins JR (1987) Identification of an E1A-inducible cellular factor that interacts with regulatory sequences within the adenovirus E4 promoter. *EMBO J* 6:4073–4081.
2. Le Cam L, et al. (2006) E4F1 is an atypical ubiquitin ligase that modulates p53 effector functions independently of degradation. *Cell* 127:775–788.
3. Sandy P, et al. (2000) p53 is involved in the p120E4F-mediated growth arrest. *Oncogene* 19:188–199.
4. Rizos H, et al. (2003) Association of p14ARF with the p120E4F transcriptional repressor enhances cell cycle inhibition. *J Biol Chem* 278:4981–4989.
5. Chagraoui J, et al. (2006) E4F1: A novel candidate factor for mediating BMI1 function in primitive hematopoietic cells. *Genes Dev* 20:2110–2120.
6. Paul C, et al. (2006) The LIM-only protein FHL2 is a negative regulator of E4F1. *Oncogene* 25:5475–5484.
7. Fenton SL, et al. (2004) Identification of the E1A-regulated transcription factor p120 E4F as an interacting partner of the *RASSF1A* candidate tumor-suppressor gene. *Cancer Res* 64:102–107.
8. Fajas L, et al. (2000) pRB binds to and modulates the transrepressing activity of the E1A-regulated transcription factor $p120^{E4F}$. *Proc Natl Acad Sci USA* 97:7738–7743.
9. Tessari MA, et al. (2003) Transcriptional activation of the cyclin A gene by the architectural transcription factor HMGA2. *Mol Cell Biol* 23:9104–9116.
10. Nojima J, et al. (2010) Dual roles of smad proteins in the conversion from myoblasts to osteoblastic cells by bone morphogenetic proteins. *J Biol Chem* 285:15577–15586.
11. Le Cam L, Lacroix M, Ciemerych MA, Sardet C, Sicinski P (2004) The E4F protein is required for mitotic progression during embryonic cell cycles. *Mol Cell Biol* 24:6467–6475.
12. Blanpain C, Fuchs E (2009) Epidermal homeostasis: A balancing act of stem cells in the skin. *Nat Rev Mol Cell Biol* 10:207–217.
13. Cotsarelis G (2006) Epithelial stem cells: A folliculocentric view. *J Invest Dermatol* 126: 1459–1468.
14. Brouard M, Barrandon Y (2003) Controlling skin morphogenesis: Hope and despair. *Curr Opin Biotechnol* 14:520–525.
15. Dotto GP (2008) Notch tumor suppressor function. *Oncogene* 27:5115–5123.
16. Candi E, et al. (2008) p63 in epithelial development. *Cell Mol Life Sci* 65:3126–3133.
17. Guerra C, et al. (2003) Tumor induction by an endogenous *K-ras* oncogene is highly dependent on cellular context. *Cancer Cell* 4:111–120.
18. Ramirez A, et al. (2004) A keratin K5Cre transgenic line appropriate for tissue-specific or generalized Cre-mediated recombination. *Genesis* 39:52–57.
19. Weiss RA, Eichner R, Sun TT (1984) Monoclonal antibody analysis of keratin expression in epidermal diseases: A 48- and 56-kd keratin as molecular markers for hyperproliferative keratinocytes. *J Cell Biol* 98:1397–1406.
20. Benitah SA, Frye M, Glogauer M, Watt FM (2005) Stem cell depletion through epidermal deletion of Rac1. *Science* 309:933–935.
21. Horsley V, Aliprantis AO, Polak L, Glimcher LH, Fuchs E (2008) NFATc1 balances quiescence and proliferation of skin stem cells. *Cell* 132:299–310.
22. Yang L, Wang L, Yang X (2009) Disruption of Smad4 in mouse epidermis leads to depletion of follicle stem cells. *Mol Biol Cell* 20:882–890.
23. Waikel RL, Kawachi Y, Waikel PA, Wang XJ, Roop DR (2001) Deregulated expression of c-Myc depletes epidermal stem cells. *Nat Genet* 28:165–168.
24. Arnold I, Watt FM (2001) c-Myc activation in transgenic mouse epidermis results in mobilization of stem cells and differentiation of their progeny. *Curr Biol* 11:558–568.
25. Barrandon Y, Green H (1987) Three clonal types of keratinocyte with different capacities for multiplication. *Proc Natl Acad Sci USA* 84:2302–2306.
26. Blanpain C, Lowry WE, Geoghegan A, Polak L, Fuchs E (2004) Self-renewal, multipotency, and the existence of two cell populations within an epithelial stem cell niche. *Cell* 118:635–648.
27. Morris RJ, et al. (2004) Capturing and profiling adult hair follicle stem cells. *Nat Biotechnol* 22:411–417.
28. Braun KM, et al. (2003) Manipulation of stem cell proliferation and lineage commitment: Visualisation of label-retaining cells in whole mounts of mouse epidermis. *Development* 130:5241–5255.
29. Jacobs JJ, Kieboom K, Marino S, DePinho RA, van Lohuizen M (1999) The oncogene and Polycomb-group gene *bmi-1* regulates cell proliferation and senescence through the *ink4a* locus. *Nature* 397:164–168.
30. Janzen V, et al. (2006) Stem-cell ageing modified by the cyclin-dependent kinase inhibitor p16INK4a. *Nature* 443:421–426.
31. Krishnamurthy J, et al. (2006) p16INK4a induces an age-dependent decline in islet regenerative potential. *Nature* 443:453–457.
32. Molofsky AV, et al. (2006) Increasing p16INK4a expression decreases forebrain progenitors and neurogenesis during ageing. *Nature* 443:448–452.
33. Signer RA, Montecino-Rodriguez E, Witte ON, Dorshkind K (2008) Aging and cancer resistance in lymphoid progenitors are linked processes conferred by p16Ink4a and Arf. *Genes Dev* 22:3115–3120.
34. Su X, et al. (2009) Rescue of key features of the p63-null epithelial phenotype by inactivation of Ink4a and Arf. *EMBO J* 28:1904–1915.
35. Martínez P, et al. (2009) Increased telomere fragility and fusions resulting from TRF1 deficiency lead to degenerative pathologies and increased cancer in mice. *Genes Dev* 23:2060–2075.
36. Flores I, Blasco MA (2009) A p53-dependent response limits epidermal stem cell functionality and organismal size in mice with short telomeres. *PLoS ONE* 4:e4934.
37. Su X, et al. (2009) TAp63 prevents premature aging by promoting adult stem cell maintenance. *Cell Stem Cell* 5:64–75.
38. Akala OO, et al. (2008) Long-term haematopoietic reconstitution by $Trp53^{-/-}$ $p16Ink4a^{-/-}p19Arf^{-/-}$ multipotent progenitors. *Nature* 453:228–232.
39. Armesilla-Diaz A, et al. (2009) p53 regulates the self-renewal and differentiation of neural precursors. *Neuroscience* 158:1378–1389.
40. Cicalese A, et al. (2009) The tumor suppressor p53 regulates polarity of self-renewing divisions in mammary stem cells. *Cell* 138:1083–1095.
41. Clayton E, et al. (2007) A single type of progenitor cell maintains normal epidermis. *Nature* 446:185–189.
42. Lechler T, Fuchs E (2005) Asymmetric cell divisions promote stratification and differentiation of mammalian skin. *Nature* 437:275–280.
43. Carroll DK, et al. (2006) p63 regulates an adhesion programme and cell survival in epithelial cells. *Nat Cell Biol* 8:551–561.
44. Serrano M, et al. (1996) Role of the *INK4a* locus in tumor suppression and cell mortality. *Cell* 85:27–37.
45. Barrandon Y, Li V, Green H (1988) New techniques for the grafting of cultured human epidermal cells onto athymic animals. *J Invest Dermatol* 91:315–318.
46. Bitoun E, et al. (2003) LEKTI proteolytic processing in human primary keratinocytes, tissue distribution and defective expression in Netherton syndrome. *Hum Mol Genet* 12:2417–2430.